Acta Cryst. (1996). D**52**, 505–517

High-Resolution Structure (1.33 Å) of a HEW Lysozyme Tetragonal Crystal Grown in the APCF Apparatus. Data and Structural Comparison with a Crystal Grown under Microgravity from SpaceHab-01 Mission

M. C. VANEY, S. MAIGNAN, M. RIÈS-KAUTT AND A. DUCRUIX*

Laboratoire de Biologie Structurale, Bâtiment 34, UMR 9920, CNRS, Université Paris-Sud, Campus du CNRS, 1 Avenue de la Terrasse, 91198 Gif sur Yvette CEDEX, France. E-mail: ducruix@cygne.lbs.cnrs-gif.fr

(Received 6 July 1995; accepted 12 December 1995)

Abstract

Crystals of tetragonal hen egg-white lysozyme were grown using Advanced Protein Crystallization Facility (APCF) apparatus under a microgravity environment (SpaceHab-01 mission) and ground control conditions. Crystals were grown from NaCl as a crystallizing agent at pH 4.3. The X-ray diffraction patterns of the best diffracting ground- and space-grown crystals were recorded using synchrotron radiation and an image plate on the W32 beamline at LURE. Both ground- and space-grown crystals showed nearly equivalent maximum resolution of 1.3–1.4 Å. Refinements were carried out with the program *X-PLOR* with final R values of 18.45 and 18.27% for structures from ground- and space-grown crystals, respectively. The two structures are nearly identical with the root-mean-square difference on all protein atoms being 0.13 Å. Some residues of the two refined structures show multiple alternative conformations. Two ions were localized into the electron-density maps of the two structures: one chloride ion at the interface between two symmetry-related molecules and one sodium ion stabilizing the loop Ser60–Leu75. The sodium ion is surrounded by six ligands which form a bipyramid around it at distances of 2.2–2.6 Å.

1. Introduction

The first X-ray structure determination of hen egg-white lysozyme (HEWL) was a tetragonal form of the enzyme (Blake, Fenn, North, Phillips & Poljak, 1962; Blake *et al.*, 1965; Phillips, 1966, 1967; Blake *et al.*, 1967; Blake, Mair, North, Phillips & Sarma, 1967). Then, the structures of triclinic, monoclinic and orthorhombic crystal forms have been determined at different resolutions and under various conditions of temperature and pressure (Table 1). Egg-white lysozyme structures from different sources are often referred to as 'lysozyme' independently of the origin and space group creating some confusion when comparisons are performed. For the sake of clarity, Table 1 summarizes parts of the data concerning egg-white lysozymes from the Brookhaven Protein Data Bank (PDB) (Bernstein *et al.*, 1977; Abola, Bernstein, Bryant, Koetzle & Weng, 1987). The purpose of this paper is to describe and compare the two high-resolution structures of HEWL from one ground-grown crystal (1.33 Å resolution data) and from one space-grown crystal (1.40 Å resolution data) and to compare them with other egg-white lysozyme structures.

The aim of a European group of protein crystal growers was to use a well characterized protein to quantify the influence of microgravity on nucleation rate, potential improvement of diffraction and mosaicity. A well characterized protein is one that has been properly defined from a biochemical (purity, ion-spray mass spectrometry) and a physical chemistry point of view (solubility diagram, X-ray structure). It was thus possible to make a calibration of the X-ray properties of ground-grown crystals to compare them with space-grown ones using identical conditions except the level of gravity. The reasons for the choice of hen egg-white lysozyme as a model protein were multiple: the structure of lysozyme is known at high resolution (Madhusudan, Kodandapani & Vijayan, 1993; Harata, 1994; Pike & Acharya, 1994; Kurinov & Harrison, 1995), it is easily available in gram quantities, it crystallizes in a time span compatible with the duration of a US Shuttle flight, its phase diagram on earth is known at various temperatures (Ataka & Asai, 1988; Howard, Twigg, Baird & Meehan, 1988; Guilloteau, Riès-Kautt & Ducruix, 1992), and it is one of the most extensively studied proteins in crystallogenesis (Feher & Kam, 1985; Ataka & Asai, 1988; Riès-Kautt & Ducruix, 1989; Mikol, Hirsch & Giegé, 1990; DeMattei & Feigelson, 1992; Monaco & Rosenberger, 1993; Forsythe & Pusey, 1994).

The Advanced Protein Crystallization Facility (APCF) apparatus was developed by the European Space Agency (ESA) and constructed by Dornier. An APCF flight unit (48 reactors) (Bosch, Lautenschlager, Potthast & Stapelmann, 1992) became available for a maiden flight on the SpaceHab-01 mission in June 1993. Four European laboratories decided to share 25 reactors of the flight unit, for a joint experiment coordinated by M. Riès-Kautt. Five series of five experiments were carried out at two different protein

Table 1. *Crystallographic and NMR data for structures available at the Protein Data Bank of egg-white lysozymes (hen, turkey, pheasant, guinea fowl, Japanese quail)*

The structures listed concern the available coordinates at the date of September 1995 at the PDB. The complexes of egg-white lysozyme with Fv or Fab fragments were deliberately omitted. For each species, the lysozyme structures are sorted by the highest symmetry, then for each space group by the highest resolution. Solvent is the number of water molecules used in the refinement. Reso is the maximum resolution data. *B* factor contains the mean temperature factor for the overall protein atoms (main and side chains) with the solvent excluded from the calculation. In case of two molecules in the asymmetric unit, two values of *B* factor are present. *B* factor is computed with the program *ACT* (Collaborative Computational Project, Number 4 (1994).

PDB code	Space group	Solvent	Reso (Å)		*R* factor (%)	*B* factor (Å^2)	References
Hen egg-white lysozyme (*Gallus gallus*)							
1LZB	$P4_32_12$	97	1.50	+Tri-*N*-acetylchitotriose	16.7	15.35	Maenaka *et al.* (1996)
1LZA	$P4_32_12$	104	1.60		16.1	17.10	Maenaka *et al.* (1996)
1HEL	$P4_32_12$	185	1.70	Recombinant form	15.2	18.79	Wilson *et al.* (1992)
1LSA	$P4_32_12$	127	1.70	120 K	20.9	22.21	Kurinov & Harrison (1995)
1LSB	$P4_32_12$	122	1.70	180 K	19.9	18.48	Kurinov & Harrison (1995)
1LSC	$P4_32_12$	105	1.70	250 K	19.5	17.62	Kurinov & Harrison (1995)
1LSD	$P4_32_12$	96	1.70	280 K	19.9	20.93	Kurinov & Harrison (1995)
1LSE	$P4_32_12$	99	1.70	295 K	19.1	22.42	Kurinov & Harrison (1995)
1LSF	$P4_32_12$	119	1.70	95 K	21.3	22.11	Kurinov & Harrison (1995)
1LSM	$P4_32_12$	170	1.70	Mutant (I55L, S91T, D101S)	16.0	25.91	Shih *et al.* (1996)
1HEW	$P4_32_12$	103	1.75	+Tri-*N*-acetylchitotriose	22.9	25.62	Cheetham *et al.* (1992)
1HEM	$P4_32_12$	185	1.80	Mutant (S91T)	14.0	22.25	Wilson *et al.* (1992)
1HEN	$P4_32_12$	185	1.80	Mutant (I55V, S91T)	15.2	18.84	Wilson *et al.* (1992)
1HEO	$P4_32_12$	185	1.80	Mutant (155V)	16.0	23.02	Wilson *et al.* (1992)
1HEP	$P4_32_12$	185	1.80	Mutant (T40S, I55V, S91T)	15.3	23.31	Wilson *et al.* (1992)
1HEQ	$P4_32_12$	185	1.80	Mutant (T40S, S91T)	15.7	22.40	Wilson *et al.* (1992)
1HER	$P4_32_12$	185	1.80	Mutant (T40S)	16.1	26.22	Wilson *et al.* (1992)
1LZC	$P4_32_12$	109	1.80	+Tetra-*N*-acetylchitotetraose	14.7	15.88	Maenaka *et al.* (1996)
1LZD	$P4_32_12$	79	1.80	Mutant (W62Y)	16.7	17.12	Maenaka *et al.* (1996)
1LZE	$P4_32_12$	106	1.80	Mutant (W62Y)+tri-*N*-acetylchitotriose	15.3	15.13	Maenaka *et al.* (1996)
1LZG	$P4_32_12$	85	1.80	Mutant (W62F)+tri-*N*-acetylchitotriose	15.9	15.27	Maenaka *et al.* (1996)
5LYT	$P4_32_12$	237	1.90	100 K	17.9	8.11	Young *et al.* (1994)
6LYT	$P4_32_12$	100	1.90	298 K	17.3	15.16	Young *et al.* (1994)
1LSY	$P4_32_12$	139	1.90	Mutant (D52S)	17.3	20.82	Hadfield *et al.* (1994)
1LSN	$P4_32_12$	177	1.90	Mutant (I55L, S91T, D101S)	15.0	27.30	Shih *et al.* (1996)
1LSZ	$P4_32_12$	126	2.00	Mutant (D52S)+product GlcNAc4	16.0	19.15	Hadfield *et al.* (1994)
2LYM	$P4_32_12$	151	2.00	1 atm, 1.4 *M* NaCl	14.9	19.81	Kundrot & Richards (1987)
3LYM	$P4_32_12$	163	2.00	1000 atm, 1.4 *M* NaCl	14.9	18.10	Kundrot & Richards (1987)
1LYZ	$P4_32_12$	97	2.00	Set W2	none	none	Diamond (1974)
2LYZ	$P4_32_12$	97	2.00	Set RS5D, different refinement	none	none	Diamond (1974)
3LYZ	$P4_32_12$	97	2.00	Set RS6A, different refinement	none	none	Diamond (1974)
4LYZ	$P4_32_12$	97	2.00	Set RS9A, different refinement	none	none	Diamond (1974)
5LYZ	$P4_32_12$	97	2.00	Set RS12A, different refinement	none	none	Diamond (1974)
6LYZ	$P4_32_12$	97	2.00	Set RS16, different refinement	none	none	Diamond (1974)
4LYM	$P4_32_12$	157	2.10	Low-humidity form	16.2	22.57	Kodandapani *et al.* (1990)
8LYZ	$P4_32_12$	0	2.50	Iodine-inactivated	none	none	Beddell *et al.* (1975)
9LYZ	$P4_32_12$	0	2.50	Nam-nag-nam substrate only	none	none	Kelly *et al.* (1979)
132L	$P2_12_12_1$	78	1.80	Reductively-methylated lysines	17.3	23.55	Rypniewski *et al.* (1993)
1RCM	$P2_12_12_1$	133	1.90	Partially reduced, carboxymethylated	18.5	24.57–23.85	Hill *et al.* (1993)
2LZH	$P2_12_12_1$	0	6.00	Cα atoms only	none	none	Artymiuk *et al.* (1982)
1LYS	$P2_1$	215	1.72	313 K	18.7	18.15–13.60	Harata (1994)
1LMA	$P2_1$	148	1.75	Low-humidity form, 2 nitrates	17.5	10.84	Madhusudan *et al.* (1993)
3LYT	$P2_1$	406	1.90	100 K	20.3	7.42–8.41	Young *et al.* (1993)
4LYT	$P2_1$	191	1.90	298 K	17.9	18.63–16.46	Young *et al.* (1993)
1LYM	$P2_1$	0	2.50		26.0	14.35–13.29	Rao *et al.* (1983)
1LZH	$P2_1$	0	6.00	Cα atoms only	none	none	Artymiuk *et al.* (1982)
1LZT	$P1$	220	1.97		25.4	10.08	Hodsdon *et al.* (1990)
2LZT	$P1$	249	1.97	5 nitrates	12.4	10.47	Ramanadham *et al.* (1990)
7LYZ	$P1$	97	2.50		none	none	Herzberg & Sussman (1983), Moult *et al.* (1976)
1HWA	NMR			NMR, minimized average	none	none	Smith *et al.* (1993)
Turkey egg-white lysozyme (*Meleagris gallopavo*)							
1TEW	$P6_122$	86	1.65		20.6	24.35	Howell (1995)
2LZ2	$P6_122$	111	2.20	Crystallized at pH = 7	19.2	42.95	Parsons (1988)
3LZ2	$P6_122$	0	2.50	LAUE method, mutant (N103D)	20.0	18.78	Howell *et al.* (1992)

Table 1 (*cont.*)

PDB code	Space group	Solvent	Reso (Å)		*R* factor (%)	*B* factor (Å^2)	References
Turkey egg-white lysozyme (*melagris gallopavo*)							
1LZ2	$P6_122$	0	2.80	Cα atoms only	none	none	Sarma & Bott (1977)
135L	$P2_1$	114	1.30		18.9	15.77	Harata (1993)
1LZ3	$P2_1$	75	1.50	Mutant (N39D, N103D)	18.4	16.14	Harata (1993)
1LZY	$P2_1$	80	1.55	+ di-*N*-acetylchitobiose	17.5	13.56	Harata & Muraki (1995)
Pheasant egg-white lysozyme (*Phasianus colchicus*)							
1GHL	$P4_32_12$	140	2.10		17.8	25.82–35.92	Lescar *et al.* (1994)
Guinea fowl egg-white lysozyme (*Numida meleagris*)							
1HHL	$P6_122$	87	1.90		17.0	18.29	Lescar *et al.* (1994)
Japanese quail egg-white lysozyme (*Coturnix coturnix japonica*)							
2IHL	$C2$	151	1.40		16.5	12.85	Houdusse *et al.* (1996)

concentrations using three different techniques, namely vapor diffusion, dialysis and free-interface diffusion. For a valid comparison of crystals grown on earth and in space it was necessary to set up an identical apparatus which experienced similar events (transportation, aging, temperature). A complete set of spare reactors, identical to the one used in flight, was filled, transported and activated in parallel with the space experiment to be used as a ground control. The flight experiments were activated during 7.5 d, but remained under microgravity for an additional 2 d before landing. Crystallization was performed by the three techniques available, with a volume of protein solution of 67 and 450 µl and identical supersaturation, calculated from the phase diagram at 291 K. The preparation, the controls and results of these experiments will be described in details elsewhere (Riès-Kautt *et al.*, 1996).

All the HEWL crystals obtained from the ground and space experiments belong to the tetragonal system $P4_32_12$. Among these crystals grown in the different reactors with different techniques, six from each set (ground control and space experiment) were chosen according to their quality and their size, and mounted into capillaries. Partial X-ray diffraction data were recorded for these crystals using synchrotron radiation (station W32, LURE) in order to measure the mosaic spread and the resolution limit, and to compare their quality. To this end, the partial data sets of the six APCF ground-grown crystals were averaged and the same procedure was applied to the six APCF space-grown crystals. Corresponding Wilson plots and I/σ curves perfectly superimpose. Therefore, using the conditions of crystallization described in this paper (temperature, pH, supersaturation) we do not observe any significant difference between space and ground crystals of the tetragonal form of HEW lysozyme. Complete comparison of the diffraction data of these crystals will be published elsewhere (Broutin, Riès-Kaut & Ducruix, 1996). Improvements in resolution were measured for all the tetragonal crystals analyzed compared with the native HEWL structures described in the PDB (Table 1). The best ground and space diffracting crystals were both grown using dialysis and complete X-ray diffraction data sets were recorded. In this paper we focus on the description of the high-resolution structure of HEWL from a ground-grown crystal (1.33 Å resolution data) and the comparison with the data and structure from a space-grown crystal (1.40 Å resolution data). The two refined structures from ground- and space-grown crystals will be then compared with other egg-white lysozyme structures.

2. Materials and methods

2.1. *Crystallization and data collection*

Throughout this study, a single batch of lysozyme chloride was used without further purification for ground and space experiments (Cat. No. L-2879, lot 51H7150, Sigma). Using denaturing gel electrophoresis and high-performance size-exclusion chromatography, it was found that it contains less than 0.3%(*w*/*w*) contaminant proteins. Purity was assessed by electrospray mass spectroscopy and gave a molecular weight of 14 306 Da (Riès-Kautt, Ducruix & Van Dorsselaer, 1994). The crystals used in this work were grown in the presence of 1.25 *M* NaCl (supersaturation 8) in the space experiment and 1.65 *M* (supersaturation 15) in the ground control condition and in 50 m*M* Na acetate buffer at pH 4.3, with a protein solution of 10 mg ml^{-1}.

As improvements in resolution were measured for a dozen of the analyzed tetragonal crystals obtained in the different reactors compared with the HEWL structures described in the PDB (Table 1), the two high-resolution diffracting crystals (the largest for the ground-grown crystal and one of the larger for the space-grown one) obtained by the dialysis technique from the ground and space experiments, were chosen to collect complete diffraction data using X-ray synchrotron radiation.

Measurements were made at 279 K on the wiggler beamline W32 (Fourme *et al.*, 1992) at LURE (syn-

Table 2. *Experimental conditions of data collection for crystals using synchrotron radiation*

Lysozyme	Ground			Space		
Number of crystals used	1			1		
Crystal size (mm)	1.1 × 1.2 × 0.6			0.7 × 0.5 × 0.5		
	Low resolution	High resolution	Cusp	Low resolution	High resolution	Cusp
Crystal-to-detector distance (mm)	160	160	160	230	160	160
X-off distance (mm)*	No translation	50	50	No translation	50	50
Oscillation angle (°)	2	1	1.5	1.5	2	1.5
Exposure time(s)/frame	10	30	30	13	30	30
Total oscillation angle (°)	90	94	45	94.5	180	45
Total exposure time(s)	450	2820	900	1890	5400	2700
Resolution (Å)	14.6–1.8	15.0–1.3	14.6–1.3	14.6–2.5	14.3–1.4	14.3–1.4
Number of reflections measured	79862	89323	43247	32726	93005	50668
R_{sym}†(%)	4.9	3.7	3.5	4.2	4.3	5.2
Number of independent reflections	10818	22485	20543	4095	21305	15860
Refined cell	78.54 78.54 37.77 90.0 90.0 90.0			78.65 78.65 37.76 90.0 90.0 90.0		
Number of independent reflections	24111 from 14.6 to 1.33 Å			21542 from 14.5 to 1.4 Å		
Completeness of data (%)	87 from 7.0 to 1.33 Å			89 from 7.0 to 1.4 Å		
$I > 3\sigma$ (%)	75.6			71.8		
R_{sym}† (%)	4.6			4.1		
$B_{overall}$ (Å^2) (Wilson)	14.7 from 15 to 1.33 Å			17.4 from 15 to 1.4 Å		
R_{merge} (ground *versus* space)	4.6 from 7.0 to 1.4 Å					

* *X*-off distance corresponds to the data sets for which a vertical translation of 50 mm along *X* axis of the image plates was applied. This allowed to get higher resolution for the collected data using small image plates. A modified version of *MOSFLM* was used to process the data with translation. † $R_{sym} = \sum |I_i - \langle I \rangle| / \sum I_i$; where I_i is the measured intensity of an individual reflection, and $\langle I \rangle$ the mean intensity of symmetry-related measurements of this reflection.

chrotron, Orsay, France) using a wavelength of 0.901 Å and a 180 mm diameter MAR Research image-plate detector. Complete diffraction data were collected with only one crystal from ground control conditions and one crystal from the space experiment. For each crystal, three data sets were collected: one at low resolution and two at high resolution (referred in Table 2 as low, high and cusp data). The weighted least-squares *R* factors on intensity for symmetry-related observations were 4.6% for the ground-grown crystal and 4.1% for the space-grown crystal. The details of the experimental conditions of data collection are shown in Table 2. As no larger image-plate system was available at the W32 station at the time of recording, the detector was offset to allow data collection at higher resolution for some of the data sets. X-ray data were processed with the program *MOSFLM* (Leslie, 1987) adapted by P. Gouet to take into account the translation of the detector.

Throughout this text, the structures of lysozyme from the ground-grown and space-grown crystals will be referred to as the ground and space structures, respectively.

2.2. *Refinement of protein structures*

The starting model for refinement of the ground-grown crystal was taken from the refined atomic coordinates (entry 6LYT) of HEW lysozyme obtained from the PDB and corresponding to the tetragonal form at 298 K (Young, Tilton & Dewan, 1994). All water molecules were removed from the initial model. This model was refined first with a rigid-body procedure and then with the conjugate-gradient facility of *X-PLOR* (Brünger, 1992*b*) using the accurate parameters described by Engh & Huber (1991). The same procedure was used for the space-grown crystal with the refined coordinates of ground-grown crystal as the starting model. All the solvent found previously for the ground structure was included in the model of the space structure and the position of each water molecule was systematically checked after each cycle of refinement. During the early stages of refinement, it was decided to include the charges on charged residues such as Lys, Arg, Asp and Glu. The free *R* test (Brünger, 1992*a*) was used to follow structure refinements. At high resolution, it proved to be extremely useful to detect abnormal behavior of the refinement. In total, 33 cycles of refinement were carried out on the ground structure and additional 14 cycles on the space structure. For the ground structure, the starting *R* factor was 42.8% (initial free *R* factor was 43.5%) before the rigid-body procedure to reach the value of 18.45% (final free *R* factor is 22.63%) at the final stage of refinement. Table 3 gives a summary of the refinement statistics for both the ground and space structures.

PEAKMAX and *WATPEAK* programs from *CCP*4 (Collaborative Computational Project, Number 4, 1994) were used to locate the water molecules at various stages of the refinement. Water molecules were inserted in the models with an initial isotropic *B* factor of 20 Å^2, if they formed at least one stereochemically reasonable hydrogen bond (between 2.6 and 3.4 Å) and were above the 3 root-mean-square (r.m.s.) level of the $|F_o| - |F_c|$ difference-density maps. They were deleted at the end of refinements if the corresponding electron density was less than the r.m.s. level of the $2|F_o| - |F_c|$ map. Water molecules with a thermal *B* factor less than three times the average *B* factor of the whole structure (protein

Table 3. *Final refinement statistics for the two lysozyme structures*

	Ground	Space
Resolution limits (Å)	7–1.33	7–1.40
R factor (%)*	18.45	18.27
R free factor (%)	22.63	22.57
No. of reflections used ($F > 0$)	23910	21276
No. of proteins atoms	1001	1001
No. of solvent molecules	142	138
No. of heteroatoms	2	2
Weighted root-mean-square deviations from ideality		
Bond lengths (Å)	0.008	0.008
Bond angles (Å)	1.478	1.480
Improper angles (°)	1.259	1.241
Dihedral angles (°)	23.26	23.47
Average *B* factors (Å^2)		
Main-chain protein atoms	14.9	16.6
Side-chain protein atoms	18.6	20.6
Overall protein atoms	16.7	18.6
Water molecules	37.6	39.9
Cl^- ion	21.4	23.5
Na^+ ion	21.0	22.4
Overall atoms (protein + water molecules + ions)	19.4	21.1

*R factor $= \sum |F_{obs} - F_{calc}| / \sum |F_{obs}|$.

atoms and solvent) were kept at the end of refinements. For the ground structure the limit was set up at 60 Å^2 while for the space structure at 65 Å^2; the difference takes into account the difference in the average *B* factor for the overall protein in the two structures (Table 3). A total of 142 and 138 water molecules were identified in the ground and space structures, respectively.

Side chains were adjusted using the $2|F_o| - |F_c|$ and the $|F_o| - |F_c|$ electron-density maps displayed with *TURBO-FRODO* (Roussel & Cambillau, 1989). Only one loop (69–71) was rebuilt from the initial model 6LYT. The carbonyl group of Pro70 had to be inverted to fit the $2|F_o| - |F_c|$ density map (Fig. 1*a*). This loop have the same conformation in the ground and space structures. Some amino acids (Lys1, Ser86 and Val109 for the two structures, plus Asn59 for the ground structure) presented alternative conformations into the density (Fig. 1*b*) with a refined occupancy of almost 50% for each position. A total of 11 side chains at the surface of the lysozyme showed disordered conformations, the density being poorly defined around some atoms of these residues. The concerned residues were: Arg21, Arg61, Trp62, Arg73, Asn77, Lys97, Asp101, Asn103, Gln121,

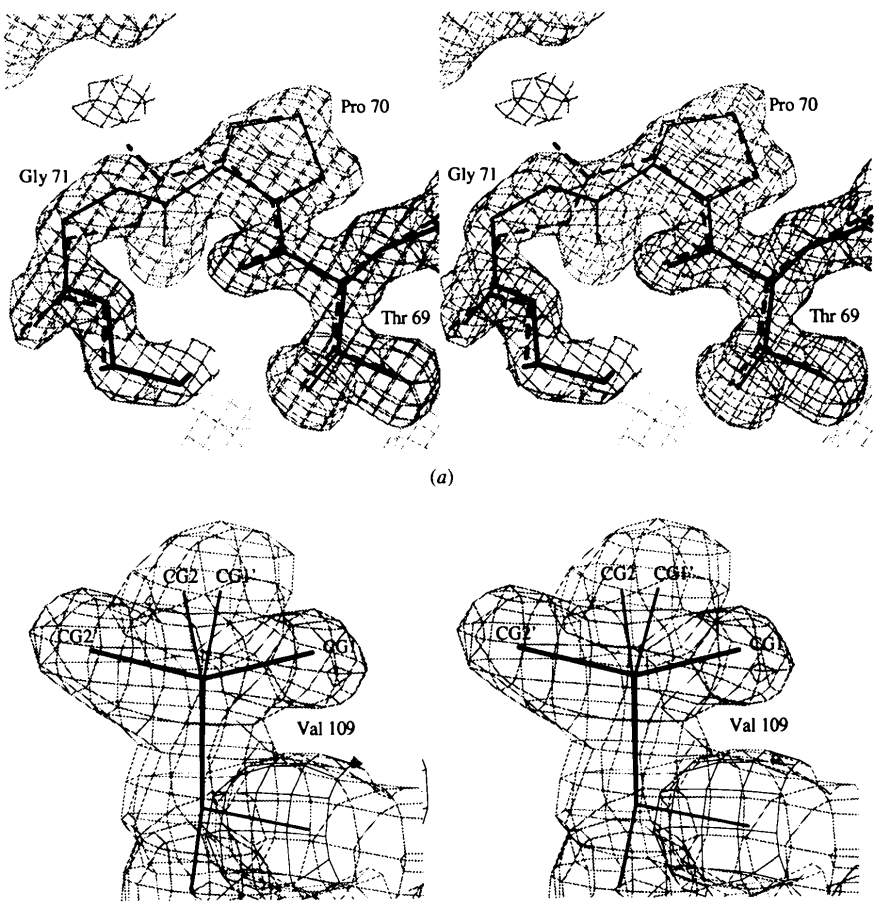

Fig. 1. Stereoscopic views for the ground structure of the final $2|F_o| - |F_c|$ electron-density map at 1.33 Å resolution with the contour level at 1σ. (*a*) The loop 69–71 was rebuilt (plain line) from the 6LYT structure (dashed line), (*b*) modeled alternative conformations for the Val109 residue.

Arg125, Leu129 for the ground structure. For the space structure the disordered side chains were the same as for ground structure except for Arg61 and Asp101 but included additional residues Asp119 and Arg128.

Some residual positive peaks appeared in the $|F_o| - |F_c|$ electron-density map near the S—S bonds, probably linked to anisotropic behavior treated as isotropic. Disulfide bridges 6–127, 30–11, 64–80, and 76–94 had torsion angles of −91.5, −70.1, 97.1 and 84.7°, respectively. The comparison of the two structures ground and space gave an overall r.m.s. difference of 0.07 Å for the main-chain atoms and 0.13 Å for the overall structures.

3. Results and discussion

3.1. *Comparison of ground and space diffraction data*

There are some generally accepted criteria for accessing to the quality of protein crystals such as the mosaic spread, the resolution limit and the evaluation of measured data as a function of resolution. The maximum resolution is the inverse value d_{min} of the largest value of the scattering vector modulus S ($S = 2\sin\theta/\lambda$) for which useful information on Bragg intensities can be extracted from a diffraction pattern recorded in given experimental conditions. At low resolution there was no difference in intensities between the two crystals. The values of B factors from the Wilson diagrams (Fig. 2*a*) were essentially estimated from about 2.0 Å to the high-resolution end of the plots. These calculated values showed a reduction in the mean isotropic B factor of almost 3 Å^2 for the ground structure (14.7 Å^2) compared to the space one (17.4 Å^2), leading to the suggestion that the space crystal is less ordered than the ground crystal. At the end of refinement, the average temperature factors of the protein atoms are 16.7 and 18.6 Å^2 for the refined ground and space structures, respectively.

The plots of the percentage of data with I/σ greater than 3σ cutoff *versus* the resolution (Fig. 2*b*) and the plot of the average I/σ *versus* the resolution (Fig. 2*c*)

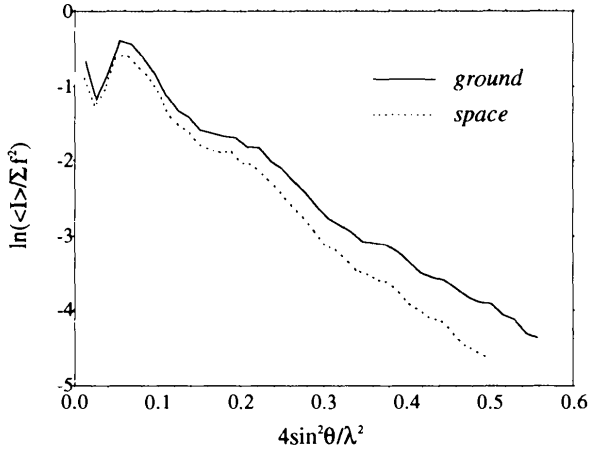

(*a*)

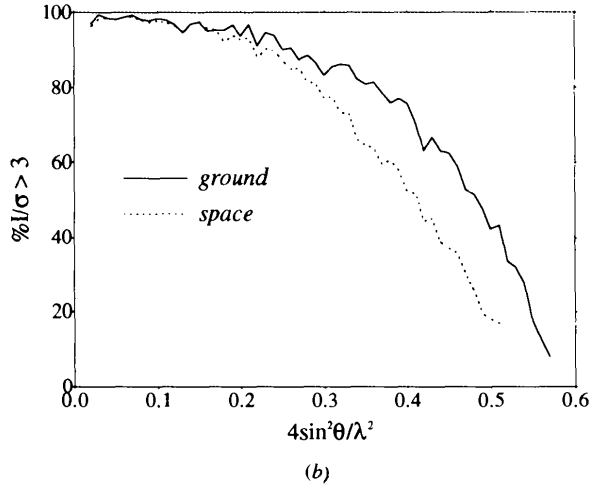

(*b*)

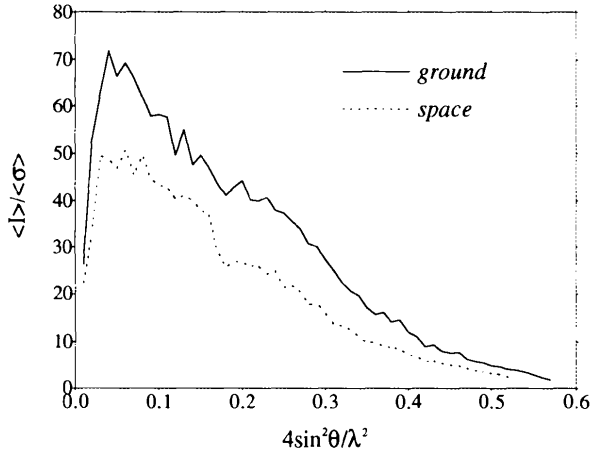

(*c*)

Fig. 2. (*a*) Wilson plots of $\ln(\langle I\rangle/\sum f^2)$ against $4\sin^2\theta/\lambda^2$. The overall B values determined from the slopes, $-2B$, of the curves are 15 Å^2 for the lysozyme structure from the ground data (plain line) and 18 Å^2 for the lysozyme structure from the space data (dashed line). (*b*) Comparison of diffraction data for ground-grown crystal and for space-grown crystal showing the percentage of $I/\sigma > 3$ as a function of $4\sin^2\theta/\lambda^2$. (*c*) Average values of I/σ plotted against $4\sin^2\theta/\lambda^2$ for the ground control crystal and for the crystal grown under microgravity.

indicate that there is some difference in diffraction data between the ground-grown crystal and the space-grown one, but no improvements can be noticed for the crystal grown under microgravity compared with the one grown on earth under the same conditions except the level of gravity.

3.2. *Accuracy of the ground and space structures*

The qualities of the ground and space structures were checked using several programs of geometry analysis such as *geomanal* (Brünger, 1992*b*), *act* (Collaborative Computational Project, Number 4, 1994) and *PROCHECK* (Laskowski, MacArthur, Moss & Thornton, 1993). For the final ground and space structures the Ramachandran plots of the main-chain torsion angles (φ and ψ) (Ramachandran & Sasisekharan, 1968) did not show any bad conformations for residues which are localized in the favored and allowed regions of the (φ,ψ) diagram. The theoretical variations of the coordinates errors were evaluated using Luzzati plots (Luzzati, 1952) and corresponded to mean positional errors of 0.15 Å for ground structure and in the range of 0.15–0.20 Å for the space structure.

3.3. *Cl^- environment*

During the refinements of the ground and space structures, a very low temperature factor was observed for a water molecule bound at the interface between two molecules of lysozyme (8 $Å^2$ in ground structure and 9.2 $Å^2$ in space one). These atomic temperature factors were lower than the average B factor of Cα atoms (14.9 $Å^2$ for ground crystal and 16.6 $Å^2$ for space crystal) and even lower than the lowest B factor of Cα (9.1 $Å^2$ for Cα of Cys30 for ground structure and 10.4 $Å^2$ for the same atom in the space structure). Furthermore, the distances were larger than expected for a strong hydrogen bond between protein atoms with a water molecule. Also, the difference Fourier electron-density map $|F_o|-|F_c|$ of this atom, considered as a water molecule, still showed a high positive peak leading to the conclusion that another atom, ion or molecule with higher scattering factor could replaced this molecule initially modeled as a water molecule.

Studies of lysozyme solutions at pH 4 by a fluorescence quenching technique (Sibille & Pusey, 1994) have shown that the number of chloride ions bound to the protein decreases when the concentration of NaCl increases. But the presence of chloride in the HEWL crystal structures is not clearly established in the literature. Phillips (1967) was the first to mention the possible interaction of three chloride ions with the protein in the tetragonal lysozyme crystal. Then, Blake, Mair *et al.* (1967) localized more precisely a putative chloride ion at the interface of two HEW lysozyme molecules (2 Å resolution data) bound to Arg114 and Ser24 of a symmetry-related molecule.

With these considerations, the water molecule previously described was replaced by a chloride ion in the ground and space structures. Then, with the use of a stronger scattering factor, no more residual positive electron-density peak in the map was present at this site. With the Cl^- occupancy factor set to 1.0, the temperature factors of the Cl^- refined to values of 21.43 $Å^2$ for ground and 23.49 $Å^2$ for space structures at the final stage of refinement. The contacts of the Cl^- with protein atoms are shown in Fig. 3 and involve the phenate of Tyr23 (the proton of this hydroxyl group can be considered as slightly positively charged), the Nδ2 of Asn113 of a symmetry-related molecule as well as a water molecule. The coordination distances of the Cl^- for the ground and space structures are listed in Table 4.

In other protein crystal structures, few chloride-binding sites have been described: in bacteriophage T4 lysozyme (1.7 Å resolution data) (Nicholson, Becktel & Matthews, 1988; Bell *et al.*, 1991), in pig pancreatic α-amylase at 2.1 Å resolution (Buisson, Duée, Haser & Payan, 1987; Qian, Haser & Payan, 1993; Larson, Greenwood, Cascio, Day & McPherson, 1994), where the Cl^- is known to activate the protein, in the deoxyhemoglobin mutant W37βR at resolution of 1.9 Å (Kavanaugh, Rogers, Case & Armone, 1992),

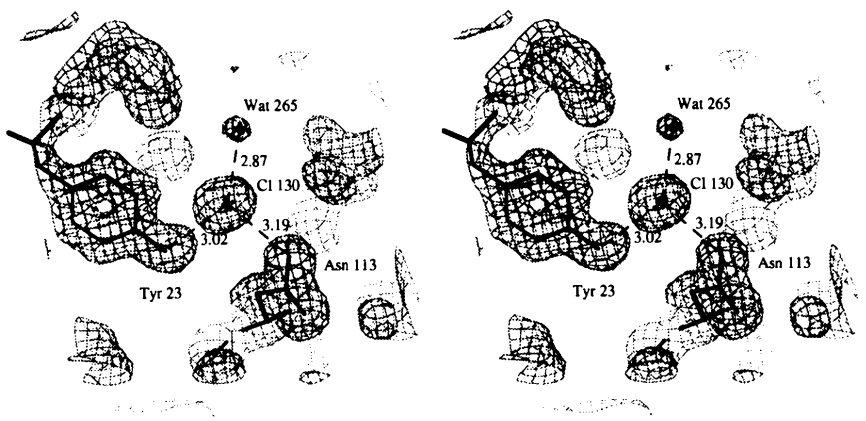

Fig. 3. Environment of the Cl^-. The phenate of Tyr23, the Nδ2 of Asn113 of a symmetry-related molecule and a water molecule are involved in the interactions with the chloride ion.

Table 4. *Coordination distances for the sodium and the chloride ions and individual thermal B factor for each atom surrounding Na^+ and Cl^- in ground and space structures*

	Ground		Space	
	Distances Na^+ (Å)	B (Å^2)	Distances Na^+ (Å)	B (Å^2)
O R73	2.56	23.1	2.62	24.9
Oγ S72	2.25	26.8	2.18	27.5
O C64	2.42	12.5	2.47	14.1
O S60	2.20	14.5	2.20	15.8
Wat 135	2.38	14.5	2.32	15.7
Wat 144	2.18	23.9	2.40	23.0
	Distances Cl^- (Å)	B (Å^2)	Distances Cl^- (Å)	B (Å^2)
OH Y23	3.02	10.6	2.93	12.3
Nδ2 N113*	3.19	12.4	3.15	13.6
Wat 265	2.87	52.2	3.05	58.2

* Atom of molecule related by the symmetry code $y-0.5$, $-x+0.5$, $z+0.25$.

in ribonuclease A (1.9 Å resolution data) (Baudet-Nessler, Jullien, Crosio & Janin, 1993), where three chloride ions were described, and in the 1.7 Å structure of dihydrofolate reductase from *E. coli* (Bolin, Filman, Matthews, Hamlin & Kraut, 1982). In all these structures, the nearest amino acids or atoms forming close contacts with Cl^- are in majority the positively charged residue Arg, the atom Nδ2 of Asn, water molecules, hydrophobic contacts, and also reported, some interactions with the atoms Oγ1 of Thr and Oγ of Ser.

3.4. *Na^+ environment*

Although Na^+ is abundant in physiological medium and is involved in the stabilization of surface charge on biological macromolecules, the interactions between Na^+ and proteins have been poorly described by X-ray crystallography because of the close values in scattering for sodium ion and a water molecule. Only high-resolution structures allow to distinguish between water molecules and sodium ion, the main argument to differentiate a sodium ion from a water molecule being the average distances between the ion and the ligands which should be close to 2.4 Å.

In the ground and space structures, the Na^+ is located in the middle of the loop Ser60–Leu75 (Fig. 4) and makes six short distances (between 2.18 and 2.62 Å) with the surrounding atoms. Fig. 5(*a*) shows the closest interaction of the Na^+ with the surrounding atoms of the protein as well as with two water molecules. The atoms concerned are the carbonyl O atoms of residues Arg73, Cys64 and Ser60, the hydroxyl O atom of Ser72 and two water molecules. The thermal B factor of these atoms as well as the coordination distances of the Na^+ are listed in Table 4 for the two lysozyme structures. In the ground and space structures, the coordination geometry of the sodium ion may be considered as a distorted octahedron (Fig. 5*b*).

An identical situation occurred with the Japanese quail egg-white lysozyme (1.4 Å resolution data; PDB code 2IHL) where a Na^+ was found at the same site, forming also a distorted octahedron with distances between 2.36 and 2.58 Å with the protein atoms and two water molecules (Houdusse, Bentley, Poljak, Souchon & Zhang, 1996).

This kind of octahedral and distorted geometry was also seen in the major grove site of a nucleic acid structure (Chevrier *et al.*, 1986). In crystallography of small organic molecules, this type of geometry is frequently observed for Na^+, showing a preference for oxygen donor ligands (Cesario *et al.*, 1993).

3.5. *Alternative conformations*

In the present work, for the ground and space structures, alternative positions for residues Lys1, Ser86 and Val109 were clearly observed without ambiguities. In addition, for the ground structure only, a second conformation for Asn59 was modeled. For all the alternative positions found in the ground and space structures, the occupancy factors were refined only at the last stage of the refinement process.

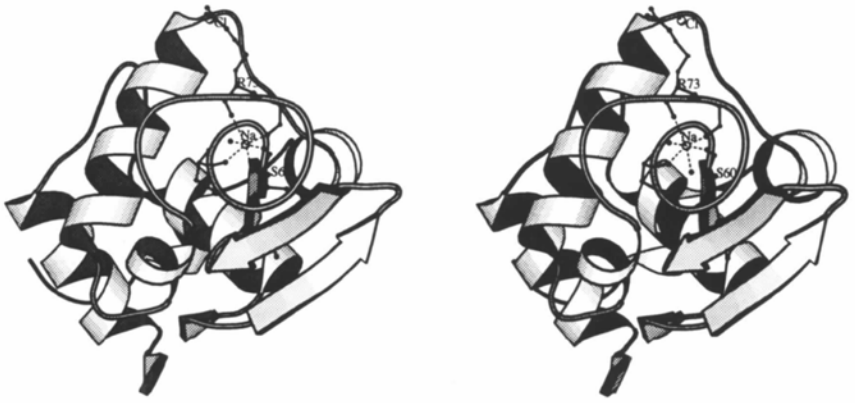

Fig. 4. Stereoview of the overall lysozyme ground structure. The Na^+ ion is located inside the loop 60–73 and the interactions are symbolized by the dashed lines. The Cl^- ion is localized at the interface of two molecules and is at a distance of about 24 Å from the Na^+ ion (for ground and space structures). All the diagrams were produced using the program *MOLSCRIPT* (Kraulis, 1991).

For residue Val109 the two alternative positions for the group Cβ, Cγ1, Cγ2 are shown in Fig. 1(*b*). Blake, Mair *et al.* (1967) first observed the alternative conformations for Val109 in the HEWL structure. They noticed that only one Cγ could be represented in the electron-density map suggesting that the group Cβ, Cγ1, Cγ2 appeared to have some rotational freedom about the Cα—Cβ bond. Alternative conformations of this residue were also described in the paper of the tetragonal crystal forms of HEWL at 1.5 Å resolution (Strynadka & James, 1991) for the native protein and for the protein bound to a trisaccharide, as well as in the HEWL mutant structure (D52S) bound with an oligosaccharide product (1.9 Å resolution data) (Hadfield *et al.*, 1994).

The side chain of Ser86 initially modeled as only one main conformation had high *B* values in the early stage of refinement (23.5 $Å^2$ for Oγ in ground structure). During the next steps of refinement the Cβ—Oγ bond appeared to be disordered and two different side-chain positions could be clearly modeled into the electron-density map. The two positions observed for Ser86 correspond to the two preferred conformations obtained for serine residues from an analysis of protein structures (Janin, Wodak, Levitt & Maigret, 1978). Serine seems to be a candidate for conformational disorder in some protein structures because of its low barrier of rotation around the Cα—Cβ bond. In the ground structure, the refined occupancy factor of the Oγ atom of Ser86 is the same ($Q_{occ} = 0.50$) for the two positions ($\chi_1 = 49$, $\chi_1' = 293.7°$). But in the space structure, the occupancies of this atom in the two conformations ($\chi_1 = 47.3$, $\chi_1' = 295.8°$) were refined to a different value ($Q_{occ} = 0.6$, $Q'_{occ} = 0.4$). In the two structures, one conformation ($\chi_1 = 49°$ for ground and $\chi_1 = 47.3°$ for space) is stabilized by an hydrogen bonding to a water molecule (distance of 2.82 Å) while no interaction seems to exist for the second alternative position of Oγ.

Spatially close to the Ser86, the residue Lys1 adopts two conformations for its terminal side-chain atoms (Cε, Nζ). In the ground structure, one of the position of Nζ atom is hydrogen-bonded with several water molecules and in interaction with Oε2 from residue Glu7; the

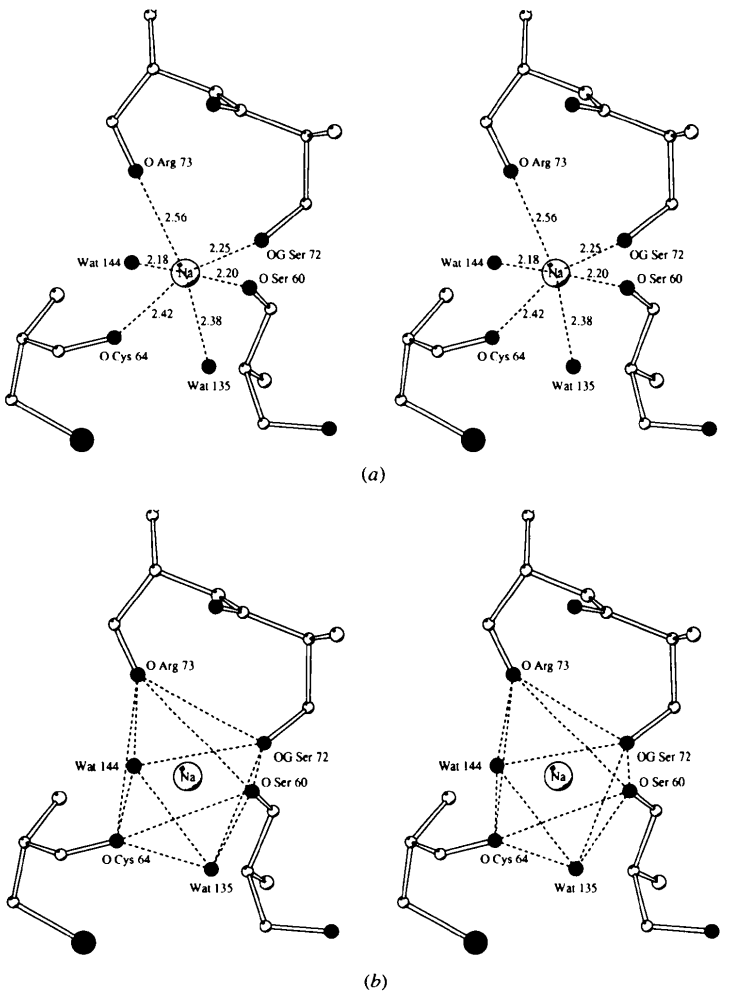

Fig. 5. Stereoviews of the sodium site in the ground structure showing the hexagonal coordination. (*a*) The short distances (between 2.2 and 2.6 Å) are particular to the Na^+ environment observed in structures of small molecules (Cesario *et al.*, 1993) and in nucleotides (Black, Huang & Cowan, 1994). (*b*) The Na^+ coordination geometry can be considered as a distorted octahedron.

other conformation of Nζ is hydrogen bonded to only one water molecule but is involved in an intramolecular salt bridge with the glutamate side chain of Glu7. In the space structure, there is no salt bridge observed at this site, the alternative positions of the Nζ atom being stabilized by hydrogen bonds with several other water molecules.

In the ground structure, the alternative positions of the group Cβ, Cγ, Oδ1, Nδ2 of Asn59 are stabilized by a number of close contacts involving two water molecules and two protein atoms (Oγ of Ser50 and Oδ1 of Asp52). In spite of the high resolution of the space structure, the two positions of Asn59 were not clearly observed into the electron-density map $2|F_o| - |F_c|$, and this residue was modeled with only one conformation.

3.6. *Comparison with other egg-white lysozymes*

Starting from the 6LYT structure, the loop Thr69–Gly71 had to be rebuilt for the ground and space structures. As shown in Fig. 1(*a*), for the ground and space structures, the peptide bond of this loop is well ordered and defined into the $2|F_o| - |F_c|$ map. It is worth pointing out that this region (loop Thr69–Gly71) is located between the residues Ser60, Cys64, Ser72 and Arg73 in contact with the Na^+. As the density of these residues is very well defined, the presence of Na^+ may stabilize the loop that becomes more ordered. Near by the loop, a water molecule localized on a twofold axis makes hydrogen bonds with the N atom of the main chain of Gly71 and its symmetry-related atom generated by the binary axis. This water molecule could also play a role in stabilizing the loop conformation especially the residues Pro70–Gly71. No other crystal packing with symmetry-related molecules involving this loop is to be noted. To be mentioned, another water molecule is localized on a binary axis, making hydrogen bonds with the Oγ of residue Thr43 and with its symmetry-related atom.

In the ground and space structures, although the electron-density map $2|F_o| - |F_c|$ of residue Trp62 is not well defined for three atoms (Cζ2, cη2 and Cζ3) of the six-membered ring, the next residue Trp63 is very well resolved as shown in Fig. 6. In the orthorhombic form of HEWL (Berthou, Lifchitz, Artymiuk & Jollès, 1983) the crystal contacts stabilize the motions of the side chain of Trp62 and the loop Pro70–Gly71. This is not the case in the tetragonal form of lysozyme. The large *B* factors observed in the ground and space structures for the Trp62 side chain compared to other Trp residues in the molecule, are consistent with the absence of electron density in the $2|F_o| - |F_c|$ map for the second ring of the residue. Trp62 is a flexible residue that may rotate in the absence of the substrate and was found almost disordered in NMR studies (Smith, Sutcliffe, Redfield & Dobson, 1993). However, it is part of the active-site cleft and involved in hydrophobic interactions with the sugar inhibitor. Upon sugar binding it moves and becomes more ordered (Kurachi, Siecker & Jensen, 1976; Perkins, Johnson, Machin & Phillips, 1978; Strynadka & James, 1991; Turner & Howell, 1995).

Conformational changes were also observed for residues Pro70–Leu75 (Perkins *et al.*, 1978; Kelly, Sielecki, Sykes, James & Phillips, 1979; Lumb, Cheetham & Dobson, 1994) and the rather flexible nature of this loop was emphasized from calculated simulations using molecular dynamics as well for free and substrate-bound lysozyme (Post *et al.*, 1986; Post, Dobson & Karplus, 1989). However, in the sugar-bound lysozyme structures, the loop Pro70–Leu75 becomes more ordered as noticed for Trp62, and in addition a flip occurs in the peptide bond between Arg73 and Asn74 (relatively to native lysozymes) (Strynadka & James, 1991; Hadfield *et al.*, 1994; Turner & Howell, 1995). The different conformations for residues Pro70–Leu75 in different crystal forms and sources of egg-white lysozyme were abundantly described (Berthou *et al.*, 1983; Turner & Howell, 1995). In the present work, the loop Ser60–Leu75 is perfectly defined into the electron-density map as well for the ground and space structures. It is not obvious to decide if the conformation of the

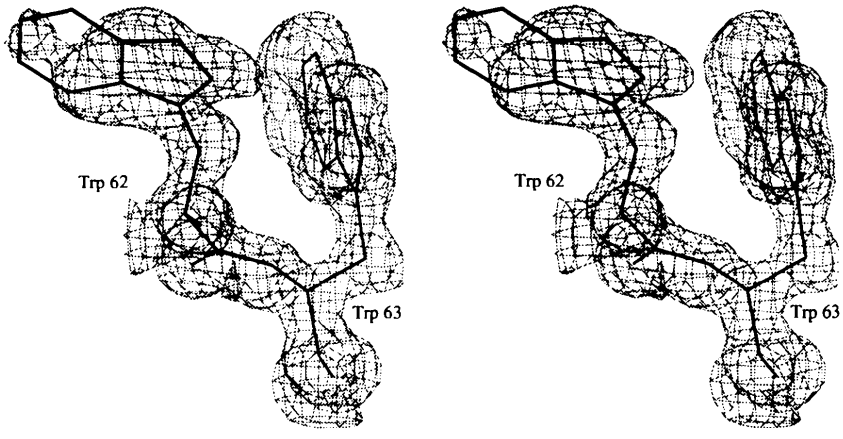

Fig. 6. Stereoscopic views for the ground structure of the final $2|F_o| - |F_c|$ electron-density map at 1.33 Å resolution with the contour level at 1σ: the missing density is observed around some atoms of the residue Trp62 while the high quality of the map shows the quasi-atomic resolution around residue Trp63. The space structure shows similar conformations and qualities of the map.

Table 5. *Comparisons of the conformations of the loop Ser60–Leu75 for the high-resolution egg-white lysozyme structures (resolution cut-off chosen at less than 2.0 Å)*

The carbonyl group of the peptide bond Arg73–Asn74 can be on the outside of the loop (toward solvent) or on the inside of the loop (rotated 180°). When there are two molecules in the asymmetric unit, they are labeled *A* and *B*. For each structure, the presence of a water molecule at the same site as Na^+ in our work (ground and space) and its number of atomic coordination are noted. $\langle B \rangle_{loop}$ is the average atomic *B* value (Å^2) of atoms of the loop Ser60–Leu75 surrounding the sodium ion or the water molecule. For comparison, $\langle B \rangle_{protein\ atoms}$, the average atomic *B* value (Å^2) of the overall protein atoms, is reported. $\Delta\langle B \rangle$ (Å^2) gives the difference between $\langle B \rangle_{loop}$ and $\langle B \rangle_{protein\ atoms}$.

PDB code	Space group	Resolution (Å)	Arg73 C=O toward solvent	Arg73 C=O rotated 180°	Presence Na^+ or H_2O	Coordination Na^+ or H_2O	$\langle B \rangle$ loop (Å^2) Ser60–Leu75	$\langle B \rangle$ (Å^2) protein atoms	$\Delta\langle B \rangle$ (Å^2)
Hen egg-white lysozyme (*Gallus gallus*)									
Ground	$P4_32_12$	1.33		×	×	6 (Na^+)	20.5	16.7	3.8
Space		1.40		×	×	6 (Na^+)	21.7	18.6	3.1
1HEL		1.70	×				24.8	18.8	6.0
1LSA		1.70		×	×	5 (H_2O)	26.1	22.2	3.9
1LSB		1.70	×				22.4	18.5	3.9
1LSC		1.70		×	No		20.5	17.6	2.9
1LSD		1.70	×				24.1	21.0	3.1
1LSE		1.70	×				25.5	22.4	3.1
1LSF		1.70	×				27.1	22.1	5.0
1HEW		1.75		×	×	6 (H_2O)	29.7	25.6	4.1
1HEM		1.80	×				28.7	22.2	6.5
1HEN		1.80	×				25.0	18.8	6.2
1HEO		1.80	×				29.4	23.0	6.4
1HEP		1.80	×				30.3	23.3	7.0
1HEQ		1.80	×				28.5	22.4	6.1
1HER		1.80	×				33.1	26.2	6.9
1LSY		1.90	×				25.1	20.8	4.3
5LYT		1.90		×	No		10.6	8.1	2.5
6LYT		1.90		×	×	6 (H_2O)	19.4	15.2	4.2
132L	$P2_12_12_1$	1.80	×				29.1	23.5	5.6
1RCM		1.90	× (*A*)				30.6 (*A*)	24.6 (*A*)	6.0 (*A*)
			× (*B*)				28.5 (*B*)	23.8 (*B*)	4.7 (*B*)
1LYS	$P2_1$	1.72		× (*A*)	× (*A*)	3 (*A*) (H_2O)	20.7 (*A*)	18.1 (*A*)	2.6 (*A*)
				× (*B*)	× (*B*)	6 (*B*) (H_2O)	18.3 (*B*)	13.6 (*B*)	4.7 (*B*)
1LMA		1.75	×				8.7	10.8	−2.1
3LYT		1.90		× (*A*)	× (*A*)	3 (*A*) (H_2O)	11.9 (*A*)	7.4 (*A*)	4.5 (*A*)
				× (*B*)	No (*B*)		14.6 (*B*)	8.4 (*B*)	6.2 (*B*)
4LYT		1.90		× (*A*)	No (*A*)		22.3 (*A*)	18.6 (*A*)	3.7 (*A*)
				× (*B*)	No (*B*)		20.7 (*B*)	16.4 (*B*)	4.3 (*B*)
1LZT	*P*1	1.97	×				11.5	10.1	1.4
2LZT		1.97	×				10.4	10.5	0.1
Turkey egg-white lysozyme (*Meleagris gallopavo*)									
135L	$P2_1$	1.30	×				15.2	15.8	0.6
1LZ3		1.50	×				15.5	16.1	−0.6
1TEW	$P6_122$	1.65	×				26.6	25.6	1.0
Japanese quail egg-white lysozyme (*Coturnix coturnix japonica*)									
2IHL	*C*2	1.40		×	×	6 (Na^+)	12.0	15.2	−3.2

loop is so well defined in the crystal that it could trap the Na^+ (or water molecule in other structures) or if the presence of Na^+ sets a specific conformation of the surrounding atoms (loop Ser60–Leu75) and is able to stabilize the loop that becomes more ordered.

To try to clarify this point, the high-resolution structures of egg-white lysozyme (resolution better than 2 Å) were divided in two classes of conformations for residues Ser60–Leu75 and especially the peptide bond Arg73–Asn74. In a general manner, when a flip occurs for the peptide bond Arg73–Asn74, the CO group of Arg73 is rotated 180° on the inside of the loop so that the Oγ of Ser72 moves away from its initial position. This change of conformation allows to capture either an ion or a water molecule. Both form hydrogen bonds with the surrounding atoms of the loop Ser60–Leu75 and sometimes with other water molecules. Among all the structures listed in Table 5 having an atom identified as a water molecule within the loop Ser60–Leu75, only 1HEW structure is a trisaccharide lysozyme complex. Thus, the presence of a water molecule within this loop does not seem characteristic of the occupancy of a bound ligand at the active site. In addition, in the partridge lysozyme structure (Turner & Howell, 1995),

a water molecule at this site was also observed in the trisaccharide-bound lysozyme. Among the 11 lysozyme molecules having the CO group of Arg73 on the inside of the loop, only six of them own a water molecule, or a Na^+ in our work, into the site. Among these, some of the water molecules (see Table 5) have a sixfold coordination which is similar to the Na^+ coordination observed in the ground and space structures.

4. Conclusions

One chloride and one sodium ion were identified in the electron-density maps of both ground and space structures but of course more ions are expected to ensure the electroneutrality of the crystal. Higher resolution data obtained with the high-brilliance source of ESRF may reveal more ions at the surface of the molecule. It was tempting to relate the better resolution (this work), to the presence of a sodium ion which could stabilize the loop Ser60–Leu75. Unfortunately, it is difficult to compare on an absolute scale the *B* factors coming from different procedures of refinement. Therefore, we have now produced crystals of tetragonal lysozyme in the absence of any cation (only H^+ are present) in order to study the conformation of loop Ser60–Leu75. Refinement is in progress (Retailleau, Riès-Kautt & Ducruix, 1996). Experiments on protein crystal growth under reduced gravity show that some protein crystals seem to benefit from microgravity. Sometimes, the space-grown crystals are larger and provide a better signal-to-noise ratio with eventually a better resolution for X-ray analysis. As far as tetragonal crystals of HEW lysozyme are concerned, after testing a dozen crystals we have not observed any improvement. Of course this does not preclude any change for the better in other crystallization conditions, for instance at low supersaturation.*

We acknowledge K. Fuhrmann, M. Chofflet, and R. Berkeljon from the European Space Agency (ESA) and the European Space Research and Technology Centre (ESTEC, Noordwijk, The Netherlands); J. Stapelmann, R. Bosch, P. Lautenschlager, K. Bockstahler (Dornier, GmbH, Friedrichshafen, Germany); the Advanced Protein Crystallization Facility (APCF) coordinator, G. Wagner (Giessen, Germany). We wish to thank the Centre National d' Etudes Spatiales (CNES), the European Space Agency (ESA) and the Centre National de la Recherche Scientifique Française (CNRS) for financial support of this project. We are indebted to N. Strynadka and M. James for kindly providing us the non deposited coordinates of their HEWL bound to a trisaccharide. We are grateful to R. Fourme and J. P. Benoit for the development of the W32 station. At last, we thank A. Leslie and P. Gouet for the adaptation of the *MOSFLM* software for the off-axis image-plate system.

* Atomic coordinates and structure factors have been deposited with the Protein Data Bank, Brookhaven National Laboratory (Reference: 193L and R193LSF, 194L and R194LSF, for the ground and space structures, respectively). Free copies may be obtained through The Managing Editor, International Union of Crystallography, 5 Abbey Square, Chester CH1 2HU, England (Reference: GR0463).

References

Abola, E. E., Bernstein, F. C., Bryant, S. H., Koetzle, T. F. & Weng, J. (1987). *Crystallographic Databases – Information Content, Software Systems, Scientific Applications*, edited by F. H. Allen, G. Bergerhoff & R. Sievers, pp. 107–132. Bonn/Cambridge/Chester: IUCr.

Artymiuk, P. J., Blake, C. C. F., Rice, D. W. & Wilson, K. S. (1982). *Acta Cryst.* **B38**, 778–783.

Ataka, M. & Asai, M. (1988). *J. Cryst. Growth*, **90**, 86–93.

Baudet-Nessler, S., Jullien, M., Crosio, M.-P. & Janin, J. (1993). *Biochemistry*, **32**, 8457–8464.

Beddell, C. R., Blake, C. C. F. & Oatley, S. J. (1975). *J. Mol. Biol.* **97**, 643–654.

Bell, J. A., Wilson, K. P., Zhang, X.-J., Faber, H. R., Nicholson, H. & Matthews, B.W. (1991). *Proteins Struct. Funct. Genet.* **10**, 10–21.

Bernstein, F. C., Koetzle, T. F., Williams, G. J. B., Meyer, E. F., Brice, M. D., Rodgers, J. R., Kennard, O., Shimanouchi, T. & Tasumi, M. (1977). *J. Mol. Biol.* **112**, 535–542.

Berthou, J., Lifchitz, A., Artymiuk, P. & Jollès, P. (1983). *Proc. R. Soc. London Ser. B*, **217**, 471–489.

Black, C. B., Huang, H. W. & Cowan, J. A. (1994). *Coordination Chem. Rev.*, **135/136**, 165–202.

Blake, C. C. F., Fenn, R. H., North, A. C. T., Phillips, D. C. & Poljak, R. J. (1962). *Nature (London)*, **196**, 1173–1176.

Blake, C. C. F., Johnson, L. N., Mair, G. A., North, A. C. T., Phillips, D. C. & Sarma, V. R. (1967). *Proc. R. Soc. London Ser. B*, **167**, 378–388.

Blake, C. C. F., Koening, D. F., Mair, G. A., North, A. C. T., Phillips, D. C. & Sarma, V. (1965). *Nature (London)*, **206**, 757–761.

Blake, C. C. F., Mair, G., North, A. C. T., Phillips, D. C. & Sarma, V. R. (1967). *Proc. R. Soc. London Ser. B*, **167**, 365–377.

Bolin, J. T., Filman, D. J., Matthews, D. A., Hamlin, R. C. & Kraut, J. (1982). *J. Biol. Chem.* **257**, 13650–13662.

Bosch, R., Lautenschlager, P., Potthast, L. & Stapelmann, J. (1992). *J. Cryst. Growth*, **122**, 310–316.

Broutin, I., Riès-Kautt, M. & Ducruix, A. (1996). In preparation.

Brünger, A. T. (1992*a*). *Nature (London)*, **355**, 472–475.

Brünger, A. T. (1992*b*). *X-PLOR Manual. Version 3.1. A System for X-ray Crystallography and NMR*. New Haven and London: Yale University Press.

Buisson, G., Duée, E., Haser, R. & Payan, F. (1987). *EMBO J.* **6**, 3909–3916.

Cesario, M., Guilhem, J., Lehn, J.-M., Méric, R., Pascard, C. & Vigneron, J.-P. (1993). *J. Chem. Soc.* **6**, 540–543.

Cheetham, J. C., Artymiuk, P. J. & Phillips, D. C. (1992). *J. Mol. Biol.* **224**, 613–628.

Chevrier, B., Dock, A. C., Hartmann, B., Leng, M., Moras, D., Thuong, M. T. & Westhof, E. (1986). *J. Mol. Biol.* **188**, 707–719.

Collaborative Computational Project, Number 4 (1994). *Acta Cryst.* **D50**, 760–763.

DeMattei, R. C. & Feigelson, R. S. (1992). *J. Cryst. Growth*, **122**, 21–30.
Diamond, R. (1974). J. *Mol. Biol.* **82**, 371–391.
Engh, R. A. & Huber, R. (1991). *Acta Cryst.* A**47**, 392–400.
Feher, G. & Kam, Z. (1985). *Methods Enzymol.* **114**, 77–112.
Forsythe, E. & Pusey, M. L. (1994). *J. Cryst. Growth,* **139**, 89–94.
Fourme, R., Dhez, P., Benoit, J.-P., Kahn, R., Dubuisson, J.-M., Besson, P. & Frouin, J. (1992). *Rev. Sci. Instrum.* **63**, 982–987.
Guilloteau, J.-P., Riès-Kautt, M. M. & Ducruix, A. F. (1992). *J. Cryst. Growth,* **122**, 223–230.
Hadfield, A. T., Harvey, D. J., Archer, D. B., MacKenzie, D. A., Jeenes, D. J., Radford, S. E., Lowe, G., Dobson, C. M. & Johnson, L. N. (1994). *J. Mol. Biol.* **243**, 856–872.
Harata, K. (1993). *Acta Cryst.* D**49**, 497–504.
Harata, K. (1994). *Acta Cryst.* D**50**, 250–257.
Harata, K. & Muraki, M. (1995). *Acta Cryst.* D**51**, 718–724.
Herzberg, O. & Sussman, J. L. (1983). *J. Appl. Cryst.* **16**, 144–150.
Hill, C. P., Johnston, N. L. & Cohen, R. E. (1993). *Proc. Natl Acad. Sci. USA*, **90**, 4136–4140.
Hodsdon, J. M., Brown, G. M., Sieker, L. C. & Jensen, L. H. (1990). *Acta Cryst.* B**46**, 54–62.
Houdusse, A., Bentley, G. A., Poljak, R. J., Souchon, H. & Zhang, Z. (1996). In preparation.
Howard, S. B., Twigg, P. J., Baird, J. K. & Meehan, E. J. (1988). *J. Cryst. Growth*, **90**, 94–104.
Howell, P. L. (1995). *Acta Cryst.* D**51**, 654–662.
Howell, P. L., Almo, S., Parsons, M. R., Hadju, J. & Petsko, G. A. (1992). *Acta Cryst.* B**48**, 200–207.
Janin, J., Wodak, S., Levitt, M. & Maigret, B. (1978). *J. Mol. Biol.* **125**, 357–386.
Kavanaugh, J. S., Rogers, P. H., Case, D. A. & Armone, A. (1992). *Biochemistry* **31**, 4111–4121.
Kelly, J. A., Sielecki, A. R., Sykes, B. D., James, M. N. G. & Phillips, D. C. (1979). *Nature (London)*, **282**, 875–878.
Kodandapani, R., Suresh, C. G. & Vijayan, M. (1990). *J. Biol. Chem.* **265**, 16126–16131.
Kraulis, P. J. (1991). *J. Mol. Biol.* **227**, 9–14.
Kundrot, C. E. & Richards, F. M. (1987). *J. Mol. Biol.* **193**, 157–170.
Kurachi, K., Siecker, L. C. & Jensen, L. H. (1976). *J. Mol. Biol.* **101**, 11–24.
Kurinov, I. V. & Harrison, R. W. (1995). *Acta Cryst.* D**51**, 98–109.
Larson, S. B., Greenwood, A., Cascio, D., Day, J. & McPherson, A. (1994). *J. Mol. Biol.* **235**, 1560–1584.
Laskowski, R. A., MacArthur, M. W., Moss, D. S. & Thornton, J. M. (1993). *J. Appl. Cryst.* **26**, 283–291.
Lescar, J., Souchon, H. & Alzari, P. M. (1994). *Protein Sci.* **3**, 788–798.
Leslie, A. G. W. (1987). *Computational Aspects of Protein Crystal Data Analysis, Proceedings of the Daresbury Study Weekend.* pp. 39–50, Daresbury, Warrington: Daresbury Laboratory.
Lumb, K. J., Cheetham, J. C. & Dobson, C. M. (1994). *J. Mol. Biol.* **235**, 1072–1087.
Luzzati, P. V. (1952). *Acta Cryst.* **5**, 802–810.
Madhusudan, Kodandapani, R. & Vijayan, M. (1993). *Acta Cryst.* D**49**, 234–245.
Maenaka, K., Matsushima, M., Song, H., Sunada, F., Watanabe, K. & Kumagai, I. (1996). In preparation.
Mikol, V., Hirsch, E. & Giegé, R. (1990). *J. Mol. Biol.* 213, 187–195.
Monaco, L. A. & Rosenberger, F. (1993). *J. Cryst. Growth,* **129**, 465–484.
Moult, J., Yonath, A., Traub, W., Smilansky, A., Podjarny, A., Rabinovich, D. & Saya, A. (1976). *J. Mol. Biol.* **100**, 179–195.
Nicholson, H., Becktel, W.J. & Matthews, B.W. (1988). *Nature (London),* **336**, 651–656.
Parsons, M. R. & Phillips, S. E. V. (1988). Protein Data Bank, entry code 2LZ2.
Perkins, S. T., Johnson, L. N., Machin, P. A. & Phillips, D. C. (1978). *Biochem. J.* **173**, 607–616.
Phillips, D. C. (1966). *Sci. Am.* **215**, 78–90.
Phillips, D. C. (1967). *Proc. Natl Acad. Sci. USA*, **57**, 484–495.
Pike, A. C. W. & Acharya, K. R. (1994). *Protein Sci.* **3**, 706–710.
Post, C. B., Brooks, B. R., Karplus, M., Dobson, C. M., Artymiuk, P. J., Cheetham, J. C. & Phillips, D. C. (1986). *J. Mol. Biol.* **190**, 455–479.
Post, C. B., Dobson, C. M. & Karplus, M. (1989). *Proteins Struct. Funct. Genet.* **5**, 337–354.
Qian, M., Haser, R. & Payan, F. (1993). *J. Mol. Biol.* **231**, 785–799.
Ramachandran, G. N. & Sasisekharan, V. (1968). *Adv. Protein Chem.* **23**, 283–437.
Ramanadham, M., Sieker, L. C. & Jensen, L. H. (1990). *Acta Cryst.* B**46**, 63–69.
Rao, S. T., Hogle, J. & Sundaralingam, M. (1983). *Acta Cryst.* C**39**, 237–240.
Retailleau, P., Riès-Kautt, M. & Ducruix, A. (1996). In preparation.
Riès-Kautt, M., Broutin, I., Ducruix, A., Shephard, W., Kahn, R., Lorber, B., Theobald, A., Giegé, R., Chayen, N., Blow, D., Paal, K. & Littke, W. (1996). In preparation.
Riès-Kautt, M. M. & Ducruix, A. F. (1989). J. *Biol. Chem.* **264**, 745–748.
Riès-Kautt, M. M., Ducruix, A. F. & Van Dorsselaer, A. (1994). *Acta Cryst.* D**50**, 366–369.
Roussel, A. & Cambillau, C. (1989). *Silicon Graphics Geometry Partner Directory*, Silicon Graphics, Mountain View, CA, USA.
Rypniewski, W. R., Holden, H. M. & Rayment, I. (1993). *Biochemistry* **32**, 9851–9858.
Sarma, R. & Bott, R. (1977). *J. Mol. Biol.* **113**, 555–565.
Shih, P., Holland, D. R. & Kirsch, J. F. (1996). In preparation.
Sibille, L. & Pusey, M. L. (1994). *Acta Cryst.* D**50**, 393–397.
Smith, L. J., Sutcliffe, M. J., Redfield, C. & Dobson, C. M. (1993). *J. Mol. Biol.* **229**, 930–944.
Strynadka, N. C. J. & James, M. N. G. (1991). *J. Mol. Biol.* **220**, 401–424.
Turner, M. A. & Howell, P. L. (1995). *Protein Sci.* **4**, 442–449.
Wilson, K. P., Malcolm, B. A. & Matthews, B. W. (1992). J. *Biol. Chem.* **267**, 10842–10849.
Young, A. C. M., Dewan, J. C., Nave, C. & Tilton, R. F. (1993). *J. Appl. Cryst.* **26**, 309–319.
Young, A. C. M., Tilton, R. F. & Dewan, J. C. (1994). *J. Mol. Biol.* **235**, 302–317.